2.5 W production at mid-rapidity

2.5.1 Introduction

The STAR experiment has recently completed in Run 9 a program, collecting data during the first collisions of polarized proton beams at a beam energy of 250GeV, giving rise to a center-of-mass energy of 500GeV. This marks the beginning of a multi-year program studying the polarization of anti-quarks inside the proton using the production of $W^{\pm}$ bosons which are produced only at an appreciable rate above ~500GeV in center-of-mass energy of colliding proton beams. This research effort has long been stressed as a key element of the RHIC Spin program [1, 2]. The first observation of $W^{\pm}$ bosons together with the Z^0 boson as the force carrier of weak interactions goes back to 1983 at the SPS at CERN and was awarded in 1984 with a Nobel prize in physics to Carlo Rubbia and Simon van der Meer. Weak interactions, in contrast to strong and electromagnetic interactions violate parity, which is a fundamental ingredient in the description of the underlying quantum theory within the Standard Model of particle physics.

In recent decades, numerous experimental results have contributed to the testing and exploration of Quantum Chromodynamics (QCD), the quantum field theory that describes quarks and gluons, also known as strong interaction. This forms the theoretical basis for the high-energy polarized proton-proton program at RHIC. It is now known that quark masses make little contribution to the mass of the proton. This mass originates mostly from the interactions mediated by the massless gluons. The strong force that confines quarks inside the proton leads to the creation of abundant gluons and quark/anti-quark pairs. These ‘silent partners’ make the dominant contribution to the mass of the proton. It is not yet completely known how the silent partners contribute to the spin of the proton.

One of the great early successes of the quark model was its apparently simple account of the spin of the proton from the spin alignment of three constituent quarks. At higher energies, however, such a simple description fails. Polarized deep-inelastic scattering (DIS) experiments, pioneered by the European Muon Collaboration, have demonstrated that the spins of all quarks and anti-quarks combined account for only about 25% of the proton spin. This finding became known as the proton spin crisis and initiated several theoretical and experimental efforts world wide to deepen our understanding of the proton spin structure. The proton's missing spin can arise from spin alignment of gluons and the orbital motion of quarks and gluons. Solving the puzzle of the proton's missing spin is essential to understand how the constituent quarks of the naive quark model are related to the actual quarks and gluons probed in high-energy experiments through high-momentum transfer probes.

A dedicated program by the PHENIX and STAR collaborations is devoted to the understanding of the gluon polarization. Results obtained by both collaborations have been included now in a first global analysis together with data from polarized deep-inelastic scattering (DIS) experiments constraining the degree to which gluons are polarized [3]. The net contribution of the gluon spin to the proton spin for momentum fraction of the gluon between 5% and 20% is

very small. This finding is dominated by data collected at RHIC by the PHENIX and STAR collaborations in polarized proton-proton collisions at a center-of-mass energy of 200GeV. Ongoing and future efforts will focus on extending current measurements at RHIC constraining the gluon spin contribution at smaller momentum fractions as low as ~0.1%. The usage of different final-state configurations in di-jet and photon-jet production at the STAR experiment employing its wide calorimetric coverage in rapidity will play an important role together with the beginning 500GeV program to extend existing measurements towards smaller gluon momentum fractions.

Correlation measurements such as di-jet production are critical to deepen our understanding on the shape of the polarized gluon distribution function, $x\Delta g(x)$, at a given gluon momentum fraction. The net gluon spin contribution, ΔG, to the proton spin is quantified by the first momentum of the polarized gluon distribution function, $\Delta G = \int \Delta g(x) dx$.

2.5.2 Mid-rapidity W program at STAR

In spite of the large body of DIS data which provided a strong constraint on the combined quark and anti-quark contribution of about 25% to the proton spin, polarized DIS measurements have important limitations. In particular, they do not directly provide information about anti-quark distributions. Hence the interest in high-energy polarized proton-proton collisions which could offer new insight, complementary to DIS using parity violating processes in polarized proton-proton collisions.

Parity violation was first discovered in β decays. The dominance of electromagnetic and strong interactions results in a rather small signal in most observed measurements in the quark sector. The collision of polarized proton beams above ~500GeV in center-of-mass energy allow to observe pure weak interactions through $W^{\pm}$ and Z^0 boson exchange and generate large parity violating single-spin asymmetries. The production of $W^{-(+)}$ bosons provides an ideal tool to study the spin-flavor structure of the proton. A Feynman graph is shown in Figure 1. $W^{-(+)}$ bosons are produced in $\bar{u} + d$ $(\bar{d} + u)$ collisions and can be detected through their leptonic decays, $e^- + \bar{\nu}_e$ $(e^+ + \nu_e)$, where only the respective charged lepton (electron/positron in the case of STAR) is measured.

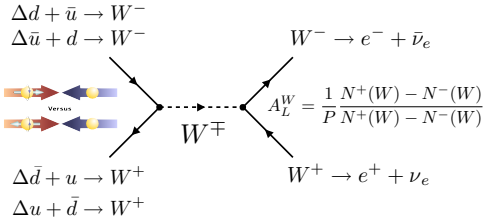

Figure 1: *Feynman diagram of W boson production. The initial-state quark couplings are shown separately for W^+ and W^- bosons.*

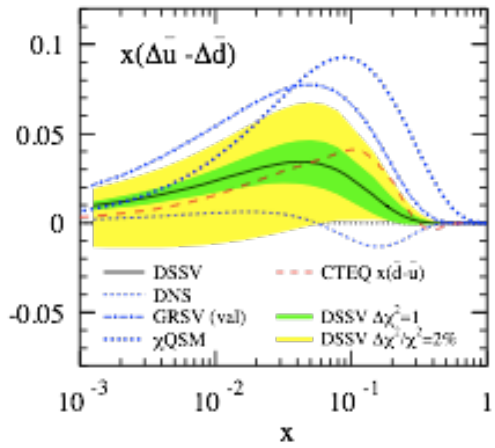

Figure 2: *Difference of polarized u-antiquark and polarized d-antiquark distribution functions as a function of x for different global fit results, DSSV, DNS and GRSV (val) [4]. The result obtained by the DSSV fit is shown together with uncertainty bands for* $\Delta\chi^2=1$ *and* $\Delta\chi^2/\chi^2=2\%$*. Also shown is a model prediction within the chiral quark soliton model. The difference of unpolarized anti-quark distribution functions as obtained by the CTEQ global analysis is shown for comparison.*

Figure 2 provides an overview of the current understanding of polarized anti-quark distribution functions, quantified as the difference of the respective anti-u ($x\Delta\bar{u}$) and anti-d ($x\Delta\bar{d}$) helicity distribution functions [4]. The DSSV global fit results in a difference of $x(\Delta\bar{u}-\Delta\bar{d})$ with a tendency to be larger than zero. A model calculation within the chiral quark soliton model also shows a positive difference. It has long been expected that non-perturbative QCD effects play an important role to account for the observed asymmetries in the production of anti-u and anti-d quarks. Various model calculations suggest an even larger difference for polarized anti-u and anti-d quarks.

The theoretical framework of extracting polarized quark and anti-quark distribution functions based on measurements of parity-violating single spin asymmetries is very well developed. This provides a firm basis to use future W production measurements in polarized proton-proton collisions at a center-of-mass energy of 500GeV in a global analysis.

The discrimination of $\bar{u}+d$ $(\bar{d}+u)$ quark combinations requires distinguishing between high p_T $e^{-(+)}$ through their opposite charge sign, which in turn requires precise tracking information. Figure 3 shows the p_T distributions at forward rapidity of the STAR EEMC acceptance (left) and at mid-rapidity of the STAR BEMC acceptance (right) in comparison to the full p_T distribution separately for W^+ and W^- bosons. The mid-rapidity distribution in the BEMC acceptance is not affected by the reduced rapidity acceptance. At forward rapidity a clear change of the p_T distribution is observed due to the underlying helicity nature of a W boson being a spin-1 particle. This effect is different for W^+ and W^- bosons. At mid rapidity, STAR will rely at first on

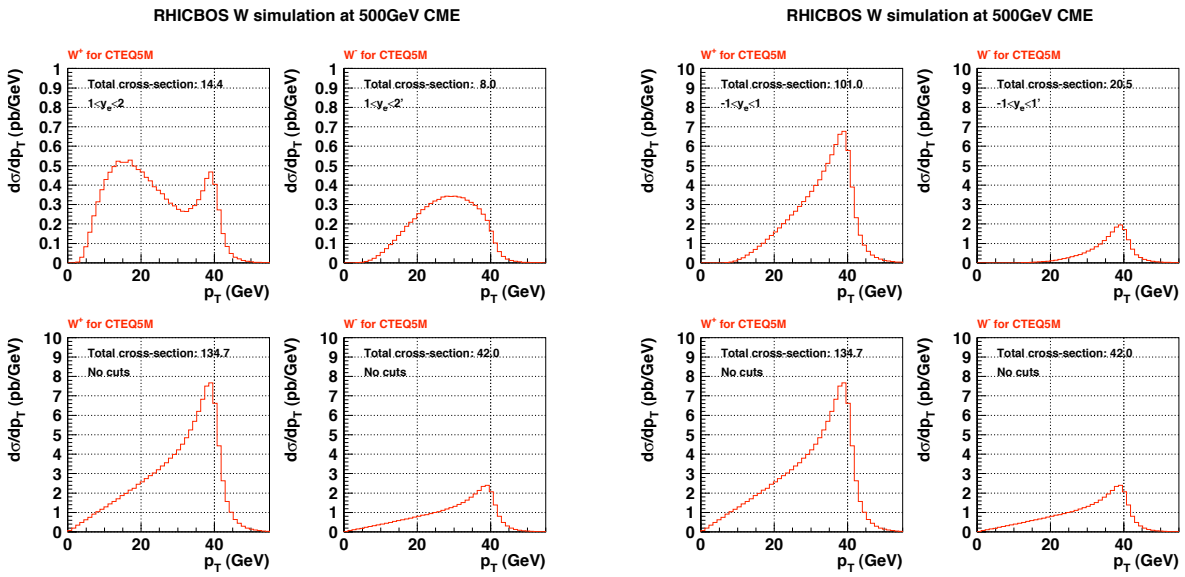

Figure 3: *Leptonic p_T cross section for W^+ and W^- case with and without a cut on the lepton rapidity of $1 < \eta_e < 2$ (left) and $-1 < \eta_e < 1$ (right), respectively based on RHICBOS [5] predictions.*

the existing Time Projection Chamber (TPC) augmented in the future by high precision inner silicon detectors. The impact of additional tracking capabilities at mid-rapidity based on the combination of the IST and SSD layers will be discussed later. At forward rapidity, new tracking capabilities will be provided by a Forward GEM Tracker (FGT) consisting of six triple-GEM detectors currently under construction.

The wide-rapidity calorimetric coverage of the STAR experiment based on the BEMC and EEMC provides an important basis to carry out a program of W production using various tools for electron/hadron discrimination.

The forward/backward rapidity region of the EEMC yields large sensitivity to polarized anti-quark distribution functions. In addition, a leading order analysis of measured asymmetries is possible in this kinematic region allowing to relate directly measured asymmetries to polarized distribution functions at leading order. In general, the ultimate extraction of polarized distribution functions will proceed through a full global analysis. In the case of STAR, this will be possible using measurements at mid-rapidity and forward/backward rapidity.

Figure 4 shows quark and anti-quark distributions for different global fit results (top) together with leptonic asymmetries as a function of the lepton rapidity for $-2.5 < \eta_e < 2.5$ (bottom) for the same set of distribution functions. It is both the forward and mid-rapidity kinematic region which provides important constraints on anti-quark distribution functions. Kinematic regions where quark polarizations dominate yield large parity violating asymmetries. This will provide an important consistency check of already well known quark distributions functions and points to

the universality nature of polarized distribution functions. Those distribution functions are probed at RHIC as shown in Figure 4 at the mass scale of the W boson mass, which is substantially larger than the scales accessible in polarized lepton-nucleon scattering experiments.

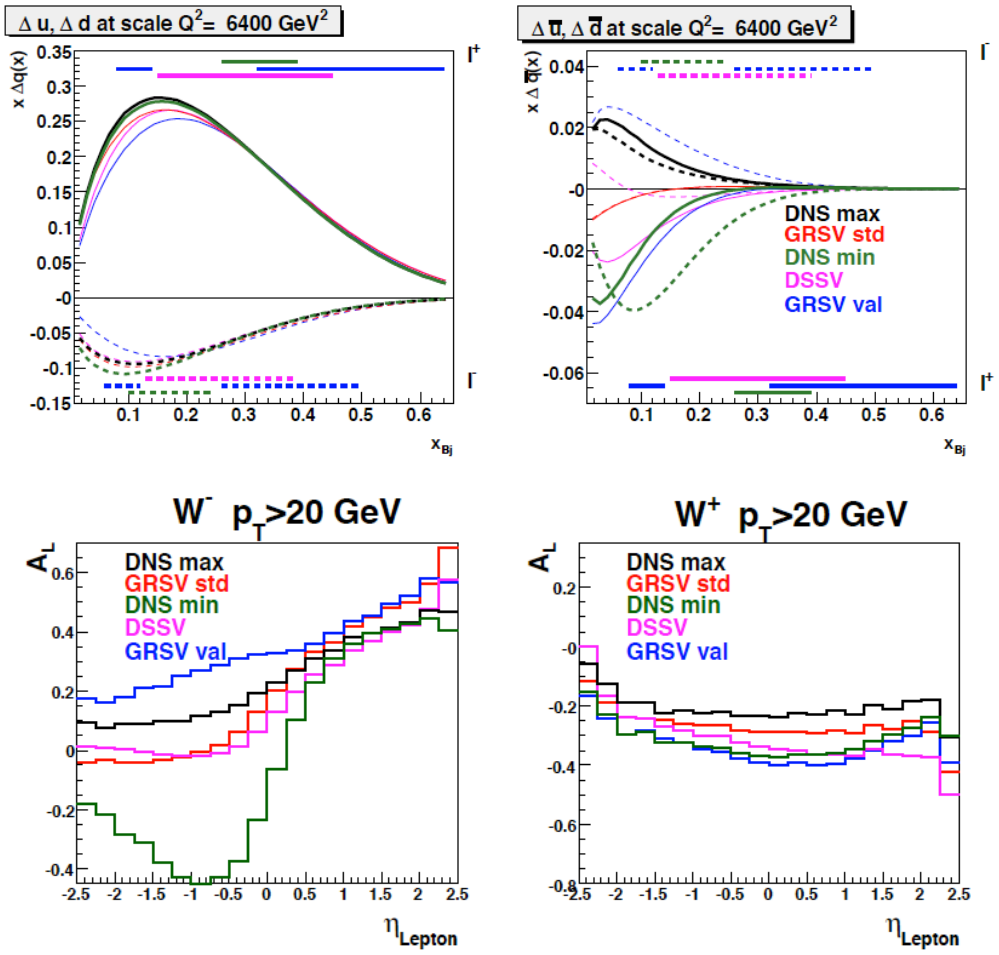

Figure 4: *Quark and anti-quark distributions for different global fit results (top) together with leptonic asymmetries as function of the lepton rapidity for -2.5 < η_e < 2.5 (bottom).*

The following sections will discuss two important aspects of W production, e/h separation and e^+/e^- charge separation. It is the charge separation at mid-rapidity where the IST/SSD combination will play a critical role.

2.5.3 Electron/Hadron separation at mid-rapidity

The yield of W boson signal events (weak interactions) over QCD background (strong interactions) is expected to be substantially smaller. The suppression of QCD background over W boson signal events by several orders of magnitude is accomplished by using the highly segmented STAR Electromagnetic Calorimeters (EMC), requiring an isolation criteria

suppressing jet events, and vetoing di-jet events based on the measured away side energy. Establishing a first W signal over QCD background is an important milestone and was a physics goal of the recently completed 500GeV data taking period in Run 9.

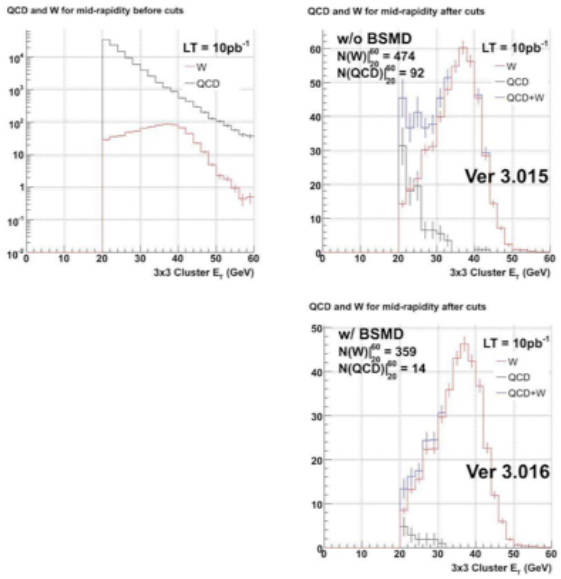

Figure 5: *Monte Carlo predictions for QCD background (QCD) and W signal (W) events before cuts (top left) and after cuts (right) as a function of the STAR Barrel Electromagnetic Calorimeter (BEMC) transverse cluster energy E_T including detector effects from a full detector GEANT simulation. All distributions are scaled to a sampled luminosity of $10pb^{-1}$. Two results are shown on the QCD background / W signal discrimination, without the Barrel Shower Maximum Detector (BSMD) (top left) and with the BSMD (bottom right). A clear Jacobian peak can be obtained even without the BSMD. The QCD background distribution is expected to be negligible at low E_T including the BSMD.*

The main physics goal of the recent 500GeV Run 9 at RHIC is the observation of a W signal over QCD background. Here, the main emphasis is placed on the observation of a Jacobian peak over QCD background without discriminating the charge sign of the W boson through a charge sign discrimination of the decay leptons, i.e. electrons versus positrons in the case of STAR. A dedicated effort has been started to simulate W signal and QCD background events using the PYTHIA event generator passed through the full STAR detector and reconstruction framework. Figure 5 shows Monte Carlo predictions for QCD background (QCD) and W signal (W) events before cuts (top left) and after cuts (right) as a function of the STAR Barrel Electromagnetic Calorimeter (BEMC) transverse cluster energy E_T including detector effects. All distributions are scaled to a sampled luminosity of $10pb^{-1}$. Two results are shown on the QCD background / W signal discrimination, without the Barrel Shower Maximum Detector (BSMD) (top left) and with the BSMD (bottom right). A clear Jacobian peak ~ $M_W/2$ can be obtained even without the BSMD. The QCD background distribution is expected to be completely negligible at low E_T

including the BSMD. The analysis of Run 9 is in full swing and first results are expected still in 2009. This provides an important baseline for the future W program at STAR, in particular the W program as discussed in this proposal of the HFT project.

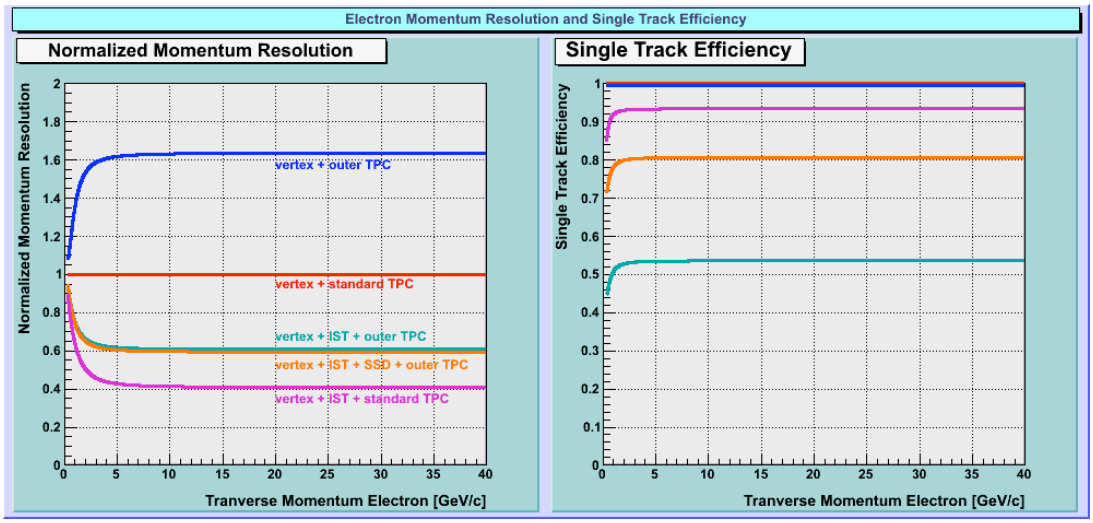

Figure 6: *Normalized momentum resolution (left) and single track efficiency (right) as a function of the electron transverse momentum for different tracking configurations: Vertex and standard TPC (outer and inner sectors) (red), Vertex and only outer TPC sectors (blue), Vertex, IST and only outer TPC sectors (green), Vertex, IST, SSD and only outer TPC sectors (orange) and Vertex, IST and standard TPC (magenta).*

2.5.4 Charge-sign discrimination at mid-rapidity

The measurement of a parity violating single spin asymmetry separately for W^+ and W^- requires the ability to efficiently separate the charge for electrons and positrons at large transverse momentum. This poses a new challenge on the understanding and calibration of the STAR TPC. A series of fast simulations have been performed using the IST/SSD combination to aid in improving the high-p_T tracking capability in addition to a vertex constraint and the TPC. For the TPC two cases have been examined. One in which all sectors (inner and outer) contribute and one in which only the outer TPC sectors contribute due to potential degraded performance at 500GeV running in polarized proton-proton collisions. This is considered to be the worst case scenario. Figure 6 shows the normalized momentum resolution as a function of the electron transverse momentum. The momentum resolution has been normalized in all cases to the Vertex plus standard TPC configuration. A drastic degradation of the momentum resolution - as expected - is found for the case where no TPC inner sectors are taken into account. This scenario is significantly improved to be even better than the Vertex plus standard TPC configuration if one adds precision hits of the IST. There is no improvement if in addition precision hits of the SSD

layer are added. This is not surprising since both layers are rather close to each other compared to the overall scales of the TPC. There is a slight improvement if one considers the Vertex plus

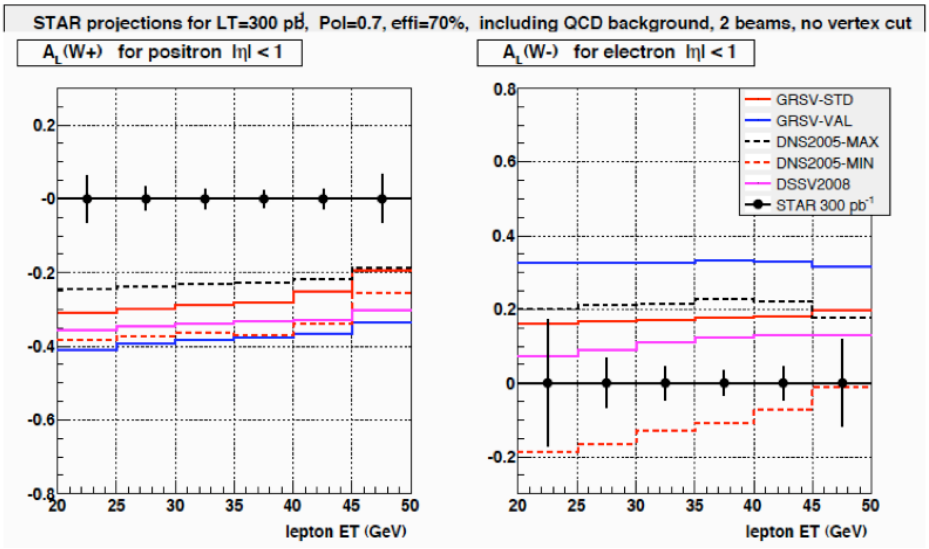

Figure 7: *Projected uncertainties for 300pb^{-1} and 70% beam polarization of A_L as a function of E_T in the mid-rapidity acceptance region of the STAR BEMC (-1<η<1).*

standard TPC configuration and adds hits of the IST. Besides the clear improvement of the momentum resolution including an IST layer in particular for a degraded TPC inner sector configuration, the single track efficiency has to be as well considered. As shown in Figure 6 (right), the single track efficiency with the IST only (similar for SSD only configuration) in addition to the Vertex and TPC configuration yields a very low efficiency. This efficiency - as expected - is to a large extend restored if one adds in addition precision hits from the SSD layers.

In summary, the combination of precision hits from the IST and SSD layers plays a critical role for efficient high-p_T track reconstruction which will be critical for the W program of charge-sign reconstruction of high-p_T electron/positron tracks in particular taking into account a degraded performance of the TPC inner sectors during 500GeV running. Here we even assumed that the TPC inner sectors are not even available at all. Again, this defines the worst possible scenario.

2.5.5 Projected performance of W production

Figure 7 shows the projected uncertainties for 300pb^{-1} and 70% beam polarization of A_L as a function of E_T in the mid-rapidity acceptance region of the STAR BEMC (-1<η<1). QCD background effects have been included and set to be equal to those determined for each E_T bin in the STAR EEMC region. It has been shown that the signal over background fraction is larger at mid-rapidity compared to at forward rapidity. This is understandable considering the shape of the p_T distribution and mid-rapidity compared to forward/backward rapidity and taking into account the fact the QCD background p_T distribution drops in both cases for larger p_T. The uncertainties

due to QCD background in Figure 7 are thus a very conservative estimate. It is expected that the mid-rapidity region will provide additional important constraints on the polarized anti-quark distributions, in particular the polarized anti-d distribution function as discussed earlier.

References:

[1] G. Bunce et al., Ann. Rev. Nucl. Part. Sci. **50**, 525 (2000).
[2] G. Bunce et al., 'Plans for the RHIC Spin Physics Program', BNL Internal Report submitted to DOE Nuclear Physics, June 2009.
[3] D. de Florian et al., Phys. Rev. Lett. **101** 072001 (2008).
[4] D. de Florian et al., 'Extraction of Spin-Dependent Parton Densities and Their Uncertainties', hep-ph 0904.3821v1.
[5] P. M. Nadolsky and C.-P. Yuan, Nucl.Phys. B666, 3 (2003), hep-ph/0304001; P. M. Nadolsky and C.-P. Yuan, Nucl.Phys. B666, 31 (2003), hep-ph/0304002.